ELSEVIER

Journal of Power Sources 66 (1997) 41–45

JOURNAL OF POWER SOURCES

Distribution of gas flow in internally manifolded solid oxide fuel-cell stacks

R.J. Boersma, N.M. Sammes *

Fuel Cell Research Group, Centre for Technology, The University of Waikato, Private Bag 3105, Hamilton, New Zealand

Received 1 August 1996; accepted 15 August 1996

Abstract

In internally manifolded fuel-cell stacks, there is a non-uniform gas flow distribution along the height of the system. To gain an insight into this distribution an analytical model has been developed. In the model, the stack is viewed as a network of hydraulic resistances. Some of these resistances are constant, while some depend upon the gas velocity and can be determined from the literature. The model consists of equations for the network with counter-current flow in the manifold channels. Only the most important resistances are included, i.e., the resistances due to splitting and combining the flows in the manifold channels, and the resistance in the gas channels of the active cell area. The ratio between the average flow and the flow in the upper cell can be solved from the model. In this manner, a very useful tool for separator-plate design is obtained.

Keywords: Fuel cells; Internal manifolding; Flow distribution; Hydraulic model; Pressure drop

1. Introduction

Fuel cells produce electricity through the electrochemical conversion of gases. Because of the high efficiency and the low emission level of pollutants, fuel cells are considered to be an environment-friendly way of producing electricity.

Depending on the load, one single fuel cell produces 0.5 to 1 V. To yield a sufficiently high voltage, the cells are stacked. This implies that, electrically, they are connected in series. Stacking of the cells imposes some difficult technological problems. For instance, reactant gases have to be able to flow on either side of each cell. This requires some spacing but that the electrical contact between each cell has to remain. Also, gases may not leak to the surroundings, or mix with the opposing gas. These functions are combined in what is usually referred to as the separator plate or interconnect.

In many cases, the separator plate also has a function in the manifolding of the feed gas and the collection of the waste gas. This is the case of internal manifolding, as opposed to external manifolding [1]. With external manifolding, a header is placed against the stack of cells and separator plates. Both these technical solutions have advantages and disadvantages, the balance of which still has to be determined.

One of the aspects of the technology of stacking of fuel cells is how well the gases distribute along a stack of fuel cells. A non-uniform distribution will cause differences in the performance of each cell, which is allowed within certain limits [1]. Important parameters in such a prediction are the actual gas flows and the resistance that the gas meets when flowing through the system.

The model presented in this paper provides an analytical approximation and is applicable for internally manifolded fuel-cell stacks. The feed gases and waste gases in the manifold channels are assumed to flow in opposite directions, which technically is the most viable option.

The analytical approach has the disadvantage that simplifications need to be made to get a result. The advantage is that under the assumptions (or simplifications), the result is verifiable, as opposed to a numerical analysis. Furthermore, the analytical approach clearly identifies the importance of each parameter in relation to the gas distribution.

2. Theory

The gas flow distribution in a fuel cell stack is determined by the hydraulic resistances in the separator plate and manifold channels. The most important resistance in the separator plate is caused by the channels adjacent to the active cell area. Other important resistances are:

* Corresponding author.

PII S0378-7753(96)02469-X

(i) the resistance caused by the flow through the manifold channels; the manifold channels can be regarded as pipes with a rough surface;

(ii) the resistance that results from the pressure drop caused by splitting of the flow in the inlet manifold channels, and

(iii) the resistance that results from the pressure drop caused by combining the flow in the outlet manifold channels.

The resistance in the channels adjacent to the cell area can be inferred from laminar flow formulae [2,5]. Flow resistance in pipes with a rough surface is described in Refs. [2–4], while resistance data for splitting and combining are given in Refs. [2,4]. The resistance depends upon the fraction that is split off or added to the mainstream in the manifold channels.

Flow results from a pressure drop. For a simple one-dimensional duct flow, the relation between flow and resistance can be given by

$$\Delta p = K\frac{1}{2}\rho v^2\frac{l}{D_h} \quad (1)$$

where Δp is the total pressure drop [1], K the hydraulic resistance coefficient, ρ the density, v the flow velocity averaged over the cross-sectional area, l the flow length, and D_h is the hydraulic diameter of the channel.

2.1. The resistance in the cell channels

The flow in these channels is assumed to be laminar. This is valid for the anode and cathode gasflow of an adiabatic solid oxide fuel cell (SOFC) with a flow length of up to 1 m, and can be checked by calculating the actual Reynolds number for a specific case.

For laminar flow, K is inversely proportional to v and, therefore, the pressure drop in Eq. (1) is linear with v [2], and hence it can be shown that

$$\Delta p_c = K_c\phi \quad (2)$$

with

$$K_c = \frac{f\eta l_c}{kA_c D_{hc}^2} \quad (3)$$

where η is the gas viscosity, k the number of channels in parallel that can be allocated to one manifold channel, l_c the corrugation length, A_c the cross-sectional area of one corrugation, D_{hc} the hydraulic diameter of one corrugation, and ϕ the flow that passes the cell area considered (which is equal to kvA_c); f is a friction factor that depends on the channel geometry. For a channel with a circular cross section $f = 32$, for a channel with a triangular cross section $f = 26.67$, and for a channel with a square cross section $f = 28.4$ [5].

[1] The sum of static, dynamic and gravitational pressures.

2.2. The resistance in the manifold channels

The pressure drop between two adjacent separator plates in the inlet and outlet manifold channels, Δp_{mi} and Δp_{mo} respectively, can be written as

$$\Delta p_{mi} = K_1\phi_i^2 \quad (4)$$

$$\Delta p_{mo} = K_2\phi_o^2 \quad (5)$$

where ϕ_i and ϕ_o are the flows in the manifold channels of the inlet and outlet, respectively.

K_1 represents the sum of the resistance of the rough pipe flow and the resistance due to splitting, while K_2 represents the sum of the resistance of the rough pipe flow and the resistance due to combining, and are described by Eqs. (6) and (7):

$$K_1 = \left(K_{mi} + K_p\frac{l_m}{D_{hm}}\right)\frac{1}{2}\frac{\rho}{A_m^2} \quad (6)$$

$$K_2 = \left(K_{mo} + K_p\frac{l_m}{D_{hm}}\right)\frac{1}{2}\frac{\rho}{A_m^2} \quad (7)$$

where K_{mi} and K_{mo} are the resistance coefficients for splitting and combination of the flow, respectively, and K_p is the resistance coefficient for the rough pipe flow of the manifold channel. These coefficients are dimensionless and are tabulated in handbooks [2,4] or have to be inferred from measurements. D_{hm} is the hydraulic diameter of the manifold channel, l_m is the distance between two separator plates, measured between the centres of the plates, and A_m is the area of a manifold channel. It is assumed that the inlet and outlet diameters are equal.

2.3. Model

The stack can be represented as a network of hydraulic resistances, in parallel and in series, as depicted in Fig. 1. In this figure, a subscript is added to the symbols used for the flow, to indicate the cell number. The convention for the symbols for pressure is analogous. It is assumed that all separator plates are of equal design and geometry.

Using Eqs. (2), (4) and (5), the pressure drop across the cell, with index j, can be written as

$$\begin{aligned} p_{1j} - p_{2j} &= K_1\{(\phi_j + \ldots + \phi_n)^2 + (\phi_{j+1} + \ldots + \phi_n)^2 \\ &\quad + \ldots + (\phi_n)^2\} + K_c\phi_n + K_2\{(\phi_n)^2 \\ &\quad + (\phi_n + \phi_{n-1})^2 + \ldots + (\phi_n + \ldots + \phi_j)^2\} \\ &= (K_1 + K_2)\sum_{m=j}^{n}\left(\sum_{i=m}^{n}\phi_i\right)^2 + K_c\phi_n \end{aligned} \quad (8)$$

The terms between the round brackets in the first line of Eq. (8) equal the local flow in the manifold inlet channel. The second line is similar but relates to the outlet channel.

In Eq. (8) it is already assumed that K_1 and K_2 are constant. Actually the parameters depend on the fraction that is split

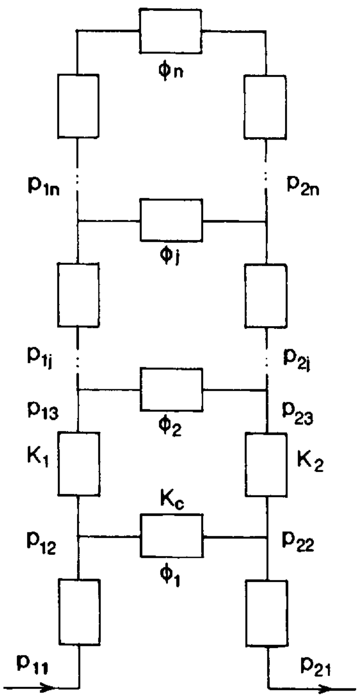

Fig. 1. Flow through a stack represented in a network. K_1 and K_2 are the inlet and outlet manifold resistances; K_c is the resistance of the corrugations; ϕ_j is the flow through the channels of cell j; p_{1j} and p_{2j} are the respective pressures at the in- and outlet of cell j.

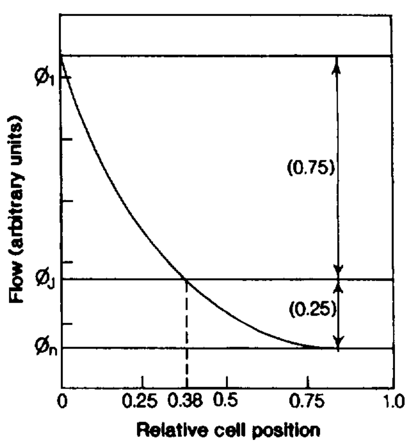

Fig. 2. Flow distribution for stacks with countercurrent manifold flow.

from, or added to, the mainstream. This fraction is small, however, and therefore approximately constant for all cells, except for the upper cells. Therefore, constant resistance coefficients are assumed. By doing this, most of the inaccuracy is introduced in the top of the stack.

To approximate the sum of the terms in Eq. (8), it is assumed that the distribution is rather good. This is done by substituting $\phi_i = \phi$, which is the average flow in cells i to n. Eq. (8) will then become

$$p_{1j} - p_{2j} = K_c\phi_n - (K_1 + K_2)\frac{\phi^2}{6}(2j^3 - \dots)\,^2 \tag{9}$$

From the network in Fig. 2, it follows that

$$p_{1j} - p_{2j} = K_c\,\phi_{j-1} \tag{10}$$

Thus, combining Eqs. (9) and (10) gives

$$\phi_{j-1} = \phi_n - \frac{K_1 + K_2}{K_c}\frac{\phi^2}{6}(2j^3 - \dots) \tag{11}$$

Assume that the average flow for the entire stack (i.e., for $i = 1$ to n) is found in cell J, then it can be written as

$$\phi_J = \frac{1}{n}\left(\sum_{j=2}^{n}\phi_{j-1} + \phi_n\right) \tag{12}$$

Substituting Eq. (11) results in

$$\phi_J = \frac{K_1 + K_2}{K_c}\frac{\phi^2}{12}[n(n^2 - 1] + \phi_n \tag{13}$$

By comparing Eq. (11), for $J = j - 1$, and Eq. (13), the cell that gets the average flow is found. Table 1 shows the number of plates and the relative location of the cell with the average flow. For stack heights of interest ($n > 100$), this is the case at approximately 38% of the stack height.

It is also now known that cell J gets the average flow. This information is required in order to determine the following flow difference ratio

$$r = \frac{\phi_J - \phi_n}{\phi_1 - \phi_n} = \frac{(2(J+1)^3 - \dots)}{n(2n^2 - 3n + 1)} \tag{14}$$

This ratio gives the quotient of the flow difference between the average and the top cell, and the bottom and the top cell.

Substituting J/n, as calculated in Table 1, gives the ratio as a function of n. In Table 2, the values of r are listed for several values of n. The latter data show that, for practical purposes, it may be assumed that $r = 0.25$. This indicates that 25% of the cells receive less than the average flow, while the remainder receive more.

Table 1
Relative position of the cell with the average flow for various stack heights, n

n	J/n
20	0.395
50	0.380
100	0.375
200	0.372
1000	0.370

Table 2
Ratio, r, for various stack heights, n. The ratio, r indicates the fraction of the cells that receive less than the average flow in the stack

n	r
20	0.289
50	0.257
100	0.247
200	0.243
1000	0.239

[2] For brevity, read for ther last term: $[2j^3 - 3j^2(2n+3) + j(6n^2 + 18n + 13) - (n+1)(2n^2 + 7n + 6)]$.

Eq. (13) can be rewritten as follows (realise that $\phi_j = \phi$)

$$\frac{\phi_n}{\phi} = 1 - \left[\frac{K_1 + K_2}{K_c}\frac{\phi}{12}n(n^2-1)\right] \tag{15}$$

The parameters on the right-hand side of Eq. (15) follow from the geometry of the separator plate and the number of cells, and the amount of gas supplied. The quotient ϕ_n/ϕ gives the ratio between the flow through the top cell and the average flow. For instance, if a flow is set for an average utilization of 80%, and may not exceed 90% utilization in the top cell, then ϕ_n/ϕ becomes 80/90 = 0.89. If a lower value is found on the right-hand side of Eq. (15), then the maximum utilization is more than 90%. This means that the number of cells must be decreased, or the geometry of the separator plate must be adapted.

3. Case study

To show the relevance of Eq. (15) a case study has been undertaken. Unfortunately, not many details of the design of separator plates are available in the open literature. Hence it was decided to use what is available, and make assumptions about the details not available. A good basis to work from was found in Refs. [6,7], where the technology of Tokyo Gas is shown.

Assume that an average utilization of 80% is targeted and that it is not wanted to exceed 90% utilization in the top cell. As indicated above, the right-hand side of Eq. (15) has to be greater than 0.89, which restricts the number of cells, *n*. Table 3 shows the data used for the calculations.

The gas flow (Table 3) was calculated on the basis of an 80% average utilization (the gas was pure hydrogen), the cell surface area was assumed to be 100 cm^2, and a current density of 1 A/cm^2 was obtained from the cell, i.e., the current density at maximum power output [7]. It should be noted that the flow has to be used at the actual temperature and pressure. The current density appears to be very high, but in Ref. [7] it is indicated that this is the direction where the technology is heading.

To calculate the pressure drop across a cell, it must be realised that the gas viscosity changes due to the electrochemistry. At the cell inlet is hydrogen, while at the cell outlet is a mixture of hydrogen and water vapour, the average composition of which is 20% hydrogen and 80% water vapour. Also depending on its location in the stack, each cell has a different outlet composition and, consequently, a different viscosity and a different value of K_c. For the calculation, the average composition and the average mix viscosity of inlet and outlet gases were used.

Taking the values in Table 3, and the above assumptions, the right-hand side of Eq. (15) reaches the critical value at a stack height of 76 cells. At this stack height, the top cell has a utilization of 90%. The cell that gets the average flow (which is at approximately 38% of the stack height) is cell no. 29, counted from the fuel gas supply side.

With the ratio *r*, it is found that the flow in the bottom cell is 1.73 times the average flow. This implies that the flow through the bottom cell is almost twice the flow through the top cell for this number of cells.

A similar calculation was made for the cathode. Assuming adiabatic operation, an average temperature increase of 150 °C, and the same critical factor as for the anode, it is found that the critical height is reached at 18 cells. The high flow required for adiabatic operation (almost 20 times stoichiometry) is the main cause for the lower cell number.

The results of the calculations depend strongly on the values of K_p, K_{mi} and K_{mo}. The values used here are tabulated in handbooks [2–5] and are related to a geometry that differs from the actual stack geometry. By actually measuring the pressure drops in a stack, however, more accurate values will be determined. These measurements can also be carried out at room temperature, ambient pressure, and using air in a stack with dummy cells.

Table 3
Data used for calculation of critical stack height for the anode gases

Symbol	Name	Value	Unit
k	channels/manifold	50	–
l_c	channel length	0.1	m
A_c	channel cross section	1×10^{-6}	m^2
D_{hc}	channel hydraulic diameter	1×10^{-3}	m
f	friction factor	28.4	–
l_m	separator plate pitch	0.005	m
D_{hm}	manifold hydraulic diameter	0.02	m
A_m	manifold cross section	3.5×10^{-4}	m^2
K_{mi}	resistsance coefficient for splitting	0.16	–
K_{mo}	resistance coefficient for combining	0.16	–
K_p	resistance coefficient for rough pipe flow	0.14	–
ϕ	flow per cell per manifold, at T and p	6.77×10^{-5}	m^3/s
ρ	average gas density, at T and p	0.074	kg/m^3
η	viscosity, at T	4.81×10^{-5}	Pa s

4. Conclusions

1. The flow distribution for fuel cell stacks can be given in analytical form, thereby a very useful tool is obtained for separator-plate design.
2. The cell that is at 38% of the stack height receives a flow that is equal to the average flow.
3. About 25% of the cells receive less than the average flow, the rest receive more.

5. List of symbols

A_c cross-sectional area of one gas channel adjacent to a cell, m^2

A_m cross-sectional area of one manifold channel, m^2

D_{hc} hydraulic diameter of one gas channel adjacent to a cell, m
D_{hm} hydraulic diameter of one manifold channel, m
f friction factor, –
k number of channels allocated to a manifold, –
K_1 resistance factor relating the effect of rough pipe flow and splitting of a flow to a pressure drop, $Pa/(m^3/s)^2$
K_2 resistance factor relating the effect of rough pipe flow and combining of flows to a pressure drop, $Pa/(m^3/s)^2$
K_c resistance factor relating laminar flow to pressure drop, $Pa/(m^3/s)$
K_{mi} resistance coefficient resulting from splitting a flow in two flows, –
K_{mo} resistance coefficient resulting from combining two flows in one, –
K_p resistance coefficient for rough pipe flow, –
l_c length of gas channel adjacent to a cell, m
l_m separator plate pitch, i.e., distance between two adjacent separator plates, measured between the plate centres, m
n number of cells in a stack, –
p pressure, Pa
v gas velocity, m/s

Greek letters

ϕ flow per cell per manifold at T and p, m^3/s
η viscosity at T, Pa s
ρ average gas density at T and p, kg/m^3

Subscripts

1 relating to the inlet manifold channel
2 relating to the outlet manifold channel
j cell number in a stack counted from the gas supply side
J cell number in a stack counted from the gas supply side that gets the average flow

References

[1] A.J. Appleby and F.R. Foulkes, *Fuel Cell Handbook*, Krieger, Malabar, FL, 1992.
[2] Verein Deutscher Ingenieure, *VDI Wärme-Atlas: Berechnungsblätter fur den Warmeübergang*, Verein Deutscher Ingenieure, Düsseldorf, 1988.
[3] W. Nunner, *Heat Transfer in Rough Pipe Tubes*, Atomic Energy Research institute, Harwell, Berks., UK, 1985.
[4] I.E. Idel'chik, *Handbook of Hydraulic Resistance, Coefficients of Local Resistance and of Friction, Moscow*, Leningrad, 1960. Translated from Russian by the Israel Program for Scientific Translations, Ltd., *IPST Cat. No. 1505*, Jerusalem, 1966, published pursuant to an agreement with the US Atomic Energy Commission and The National Science Foundation, Washington, DC., *AEC-TR-6630*, reproduced by the US Department of Commerce, National Information Service, Springfield, VA, USA.
[5] W.M. Kays and A.L. London, *Compact Heat Exchangers*, McGraw-Hill, New York, 1964.
[6] M. Hishinuma, T. Kawashima, I. Yasuda, Y. Matsuzaki and K. Ogasawara, Current status of planar type SOFC development at Tokyo Gas, *2nd European Solid Oxide Fuel Cell Forum, Oslo, Norway, 6–10 May 1996*, p. 185.
[7] M. Hishinuma, T. Kawashima, I. Yasuda, Y. Matsuzaki, K. Ogasawara and T. Ogiwara, Development of a 1 kW-class planar type SOFC at Tokyo Gas, *1st European Solid Oxide Fuel Cell Forum, Lucerne, Switzerland, 3–7 Oct. 1994*, p. 953.